Original Article

Differential adhesion and fibrinolytic activity of mesenchymal stem cells from human bone marrow, placenta, and Wharton's jelly cultured in a fibrin hydrogel

Journal of Tissue Engineering
Volume 10: 1–17

DOI: 10.1177/2041731419840622
journals.sagepub.com/home/tej
SAGE

Casandra P Chaires-Rosas[1], Xóchitl Ambriz[2], Juan J Montesinos[3], Beatriz Hernández-Téllez[1], Gabriela Piñón-Zárate[1], Miguel Herrera-Enríquez[1], Érika Hernández-Estévez[3], Javier R Ambrosio[2] and Andrés Castell-Rodríguez[1]

Abstract

Mesenchymal stem cells isolated from different tissues should share associated markers and the capability to differentiate to mesodermal lineages. However, their behavior varies in specific microenvironments. Herein, adhesion and fibrinolytic activity of mesenchymal stem cells from placenta, bone marrow, and Wharton's jelly were evaluated in fibrin hydrogels prepared with nonpurified blood plasma and compared with two-dimensional cultures. Despite the source, mesenchymal stem cells adhered through focal adhesions positive for vinculin and integrin αV in two dimensions, while focal adhesions could not be detected in fibrin hydrogels. Moreover, some cells could not spread and stay rounded. The proportions of elongated and round phenotypes varied, with placenta mesenchymal stem cells having the lowest percentage of elongated cells (~10%). Mesenchymal stem cells degraded fibrin at distinct rates, and placenta mesenchymal stem cells had the strongest fibrinolytic activity, which was achieved principally through the plasminogen–plasmin axis. These findings might have clinical implications in tissue engineering and wound healing therapy.

Keywords

Human mesenchymal stem cells, fibrin, adhesion, fibrinolysis

Received: 13 December 2018; accepted: 8 March 2019

Introduction

Tissue engineering and regenerative medicine is an evolving field with the aim of repairing the structure and functions of tissues and organs by generating tissue substitutes. These substitutes are formed by cells, chemical signals, and scaffolds.

Mesenchymal stem cells (MSCs) are good candidates for this purpose because they can accelerate tissue repair.[1–3] To accomplish this goal, they may be able to differentiate into mesodermal, ectodermal, and endodermal lineages, and modulate repair processes by paracrine signaling.[4–8]

MSCs were first isolated from bone marrow (BM), and the International Society for Cellular Therapy (ISCT) established the criteria that MSCs must fulfill.[9] MSCs should adhere to plastic substrates and exhibit a spindle or fibroblastoid shape; differentiate in vitro to osteoblasts, adipocytes, and chondroblasts; and have the following phenotypes: CD105+, CD90+, CD73+, CD45–, CD34–, CD14 or CD11b–, CD79α or CD19–, and HLA-DR–.

[1]Department of Cellular and Tissue Biology, Faculty of Medicine, National Autonomous University of Mexico, Mexico City, Mexico
[2]Department of Microbiology and Parasitology, Faculty of Medicine, National Autonomous University of Mexico, Mexico City, Mexico
[3]Oncology Research Unit, Oncology Hospital, National Medical Center, Mexican Social Security Institute, Mexico City, Mexico

Corresponding author:
Andrés Castell-Rodríguez, Department of Cellular and Tissue Biology, Faculty of Medicine, National Autonomous University of Mexico, Avenida Universidad 3000, 04510 Ciudad de México, Mexico.
Email: castell@unam.mx

Since then, they have been isolated from different tissues, and many other markers and characteristics have emerged. They have been obtained from adipose tissue (AT), dental pulp, placenta (PL), and umbilical cord, and it is assumed that they possess similar characteristics.[10–12]

BM-MSCs are the most studied MSCs in tissue engineering and regenerative medicine as well as in three-dimensional (3D) culture. The isolation of MSCs from PL and Wharton's jelly (WJ) tissue would have several practical advantages over BM, including procurement of tissue samples, reduced donor damage, and feasibility of storing large quantities of MSCs for future stem cell–based therapy and tissue engineering. This work explores whether MSCs isolated from BM, PL, and WJ share the same behavior in a 3D context using fibrin hydrogels. Fibrin is the terminal product of the coagulation cascade in response to blood vessel injury and is the natural matrix in all cases of wounds; thus, it has been long used as a scaffold for tissue engineering.[13,14] Fibrin hydrogel has been used as a delivery system for autologous BM-MSCs to accelerate chronic and acute cutaneous wound healing in both murine models and clinical cases.[1] Today, fibrin hydrogels are generated with purified fibrinogen from blood plasma, as it is the best way to control fibrinogen and thrombin concentrations, hydrogel polymerization, and structure.[15,16] Different groups have reported that MSCs embedded in this system can adhere, proliferate, migrate, and differentiate.[15–18] Nevertheless, it lacks other plasma constituents, making it necessary to use nonpurified plasma to better understand the interactions between cells and this natural scaffold. Despite existing genetic diversity among humans, the composition and concentration of coagulation factors in samples from healthy donors is similar,[19] which aids in obtaining reliable results in vivo in tissue engineering and regenerative medicine.[20,21]

Cellular adhesion in two-dimensional (2D) models has been well studied, and structures such as focal adhesions (FAs) have been characterized. Nonetheless, these structures might not be the same in composition and functionality in 3D,[22] as adhesion is affected by scaffold mechanics and chemical components. FAs permit communication between cells and their extracellular matrix (ECM)/scaffold through mechanotransduction. Vinculin is a vital protein for mechanotransduction in 2D and participates in the linkage between the actin cytoskeleton and specific receptors, such as integrins, after adhesion to a substrate. The vinculin presence in FAs regulates direction and cell polarity during migration in 2D and 3D cultures.[23] Because fibrin has arginine–glycine–aspartic acid (RGD) sequences, it is expected that MSCs adhere to it via FAs. Hakkinen et al.[24] demonstrated that fibroblasts seeded in fibrin hydrogels expressed vinculin and β1 integrin in FA, a situation that has not been evaluated in different types of MSCs.

MSCs ability to degrade a scaffold has been related to their adhesion and differentiation. Khetan et al.[25] observed that BM-MSCs needed to hydrolyze methacrylated hyaluronic acid (MeHA) hydrogel to generate cellular traction and to be able to differentiate toward an osteoblastic lineage rather than an adipocytic one. Plasmin is the major fibrinolytic enzyme, and BM-MSCs express the enzymes that regulate its activity, such as tissue and urokinase plasminogen activators (tPA, uPA), urokinase plasminogen activator receptor (uPAR), and plasminogen activator inhibitor 1 (PAI-1).[26,27] PAI-1 expression is related to the migratory capability of BM-MSCs, WJ-MSCs, and PL-MSCs.[28] Nevertheless, their fibrinolytic activities were not compared.

In this work, BM-MSCs, PL-MSCs, and WJ-MSCs were seeded in fibrin hydrogels from nonpurified blood plasma, and their adhesion was evaluated through the analysis of the presence of FA proteins (vinculin and integrin αV) and their fibrinolytic capability in the presence of specific inhibitors.

Materials and methods

Isolation of MSCs

MSCs were isolated from human BM, PL, and WJ, which were collected by donation under written informed consent. Tissue samples from BM (n = 3), PL (n = 3), and WJ from umbilical cord (n = 3) were obtained under ethical guidelines from Hospitals Bernardo Sepúlveda, National Medical Center (NMC), Francisco del Paso y Troncoso of the Mexican Social Security Institute (IMSS), and Eduardo Liceaga General Hospital, respectively.

MSCs from PL and BM were isolated in accordance to protocols previously described elsewhere.[29] Briefly, BM-MSCs were obtained by density gradient and posterior plastic adherence of mononuclear cells. PL-MSCs were obtained by mechanical and enzymatic digestion with trypsin for 30 min at 37°C. Isolated cell pellets were resuspended in Dulbecco's Modified Eagle Medium Low Glucose (DMEM-LG) supplemented with fetal bovine serum (FBS) 10%, L-glutamine 4 mM, and antibiotics (penicillin 100 U/mL, streptomycin 100 mg/mL and gentamicin 100 mg/mL), all from Gibco BRL (Rockville, MD, USA). Cells were seeded at a density of 2×10^5 cells/cm^2. Four days after isolation, nonadherent cells were removed, and fresh medium was added. When cells reached 80% confluence, the cell monolayer was detached (trypsin 0.05%, ethylenediaminetetraacetic acid (EDTA) 0.02%) and reseeded to a density of 2×10^3 cells/cm^2.

MSCs from umbilical cord were obtained from WJ using an explant protocol-modified from a previous one.[30] Blood vessels were removed from the sample, and it was sectioned in final fragments of 1 cm^2. Explants were cultured in Dulbecco's Modified Eagle Medium Nutrient Mixture F12 (DMEM-F12) supplemented with FBS 10%, L-glutamine 4 mM, and antibiotics (penicillin 100 U/mL, streptomycin 100 mg/mL, and gentamicin 100 mg/mL), all from Gibco

BRL. Media were changed every third day up to 2 weeks, when the explants were removed. When cells reached 80% confluence, the cell monolayer was detached (trypsin 0.05%, EDTA 0.02%) and reseeded to a density of 2×10^3 cells/cm^2.

Characterization of MSCs

Immunophenotypic characterization and mesodermal differentiations were performed as previously described.[29] The presence of MSCs markers (CD105, CD90, CD73, CD13, and HLA-ABC) and absence of CD34, CD45, CD14, CD31, and HLA-DR were detected by flow cytometry analysis with monoclonal antibodies coupled to fluorescein isothiocyanate (FITC), phycoerythrin (PE), and allophycocyanin (APC) from BD Biosciences (San Diego, CA, USA) in cell passages 1 to 4. Stained cells were evaluated with a FACS CANTO II Flow Cytometer (BD Biosciences) with at least 10,000 events per sample, and the data were analyzed with FlowJo 10 software (FlowJo LLC, Ashland, OR, USA).

Adipogenic differentiation was induced by the stem cell commercial kit MesenCult Adipogenic Differentiation Kit, supplemented with stimulatory supplements (Stemcell Technologies, Inc., Vancouver, BC, Canada) for 14 days, and confirmed by Oil Red O Staining (Sigma-Aldrich, St. Louis, MO, USA), counterstained with hematoxylin to allow visualization of nuclei. Osteogenic differentiation was induced by the stem cell commercial kit MesenCult Osteogenic Differentiation Kit, supplemented with 10^{-8} M dexamethasone, 0.2 mM ascorbic acid, and 10 mM β-glycerol phosphate (Stemcell Technologies, Inc.) for 21 days, and confirmed by alkaline phosphatase staining (Sigma-Aldrich). Chondrogenic differentiation was induced with the commercial kit Chondrocyte Differentiation Medium BulletKit consisting of chondrogenic differentiation basal medium supplemented with SingleQuots of dexamethasone, ascorbate, Insulin–Transferrin–Selenium (ITS) supplement, sodium pyruvate, proline, and L-glutamine (Cambrex-Lonza BioScience, Walkersville, MD, USA) supplemented with 10 ng/mL TGF-β3 (Cambrex-Lonza BioScience) for 28 days. Chondrogenesis was confirmed through Alcian blue staining (Sigma-Aldrich).

MSCs culture in fibrin hydrogels

Samples of human plasma from healthy donors were provided by the blood bank of General Hospital of Iguala, Guerrero, Mexico from the Institute for Social Security and Services for State Workers (ISSSTE). Plasma was obtained by primary fractioning of total blood. Fibrin hydrogels were prepared from nonpurified plasma of individual donors. A fibrin suspension of 200 μL was prepared with 136 μL of plasma, 24 μL of NaCl 0.9%, 40 μL of $CaCl_2$ 1%, and 2500 cells, and then incubated at 37°C for 30 min to induce polymerization. Subsequently, DMEM-LG supplemented medium was added to PL-MSCs and BM-MSCs fibrin gels, and DMEM-F12 supplemented medium was added to WJ-MSCs gels. As controls, 7500 cells/cm^2 were seeded on glass coverslips coated with poly-L-lysine (Sigma-Aldrich).

Immunofluorescence staining

Viability was analyzed in hydrogels and monolayers cultured for 3 days through calcein and ethidium homodimer stains (LIVE/DEAD Kit, Thermo Fisher Scientific, Waltham, MA, USA) according to the instructions of the manufacturer. Death control was achieved by treating cells of both conditions with ethanol for 30 min before staining. Panoramic images (100×) were taken using a Nikon Eclipse 80i microscope (Nikon, Shinagawa, Tokyo, Japan) with NIS-Elements F4 software (Nikon). For viability estimation, cells were counted manually, since it was difficult to delimitate cell boundaries in fibrin hydrogel cultures with a software.

Vinculin and integrin αV proteins were detected after culture in fibrin hydrogels and monolayers on glass coverslips. Cells cultured for 0.5, 12, 24, 48, and 72 h were fixed with formaldehyde 4% for 10 h (hydrogel) and 30 min (monolayer). Hydrogels were immersed in Tissue Tek OCT compound (Sakura Finetek, Torrance, CA, USA), frozen at −80°C, and cryo-sectioned. Samples (monolayers and cryo-sections) were permeabilized with Triton X-100 0.1% (10 min for monolayers, 15 min for cryo-sections) and incubated with phosphate - buffered saline (PBS) albumin 5% for 30 min. Primary antibody for anti-vinculin 1:100 (kit FAK-100, Merck-Millipore, Burlington, MA, USA) and its secondary antibody anti-mouse-CY5 1:200 (Seracare, Milford, MA, USA) were used. Cryo-sections from fibrin hydrogels and monolayers cultured for 48 h were also incubated with anti-CD51 1:75 (Enzo Biochem, Farmingdale, NY, USA) and its secondary antibody anti-rabbit-FITC 1:200 (Merck-Millipore). Samples were incubated with each antibody for 1 h at room temperature. Subsequently, samples were incubated with phalloidin-TRITC 1:1000 (kit FAK-100, Merck-Millipore) for 30 min and DAPI (kit FAK-100, Merck-Millipore) for 10 to 15 min (monolayer or cryo-sections, respectively). Samples were mounted with DAKO solution (Agilent Technologies, Sta. Clara, CA, USA). Some cryo-sections were stained with primary antibody anti-CD105 1:200 (Invitrogen, Carlsbad, CA, USA) in a quadruple stain with anti-vinculin, phalloidin-tetramethylrhodamine (TRITC), and 4',6-diamidino-2-phenylindole (DAPI). The secondary antibody used for anti-CD105 detection was anti-mouse-FITC 1:100 (Merck-Millipore). Panoramic images (200×) were taken using a Nikon Eclipse 80i microscope; Z stacks (630×, 400×) were acquired using Leica TCS SP5—Leica TCS SP8 confocal microscopes with LASX software (Leica Microsystems GmbH, Wetzlar, Germany).

Fibrinolysis analysis

Enzymatic degradation of fibrin hydrogels was evaluated at low cell density (1500 cells/mL) in the presence or absence of fibrinolytic inhibitors: aprotinin 200 μg/mL (Sigma-Aldrich), BB-94 5 μM (Abcam, Cambridge, UK), tranexamic acid 400 μg/mL (Sigma-Aldrich), aprotinin/tranexamic acid, aprotinin/BB-94, and BB-94/tranexamic acid for 7 days. Inhibitors were added to the fibrin mix before polymerization. Degraded zones were imaged in an Olympus SZX7 stereoscopic microscope (Shinjuku, Tokyo, Japan).

Image processing

Micrographs were analyzed through Fiji-ImageJ 1.51h ((National Institutes of Health, (NIH), Bethesda, MD, USA) software. Micrographs were edited to adjust brightness, contrast, and color using the same magnitudes for each assay. Z stacks were processed in two ways: maximally projected to generate 2D images or 3D video reconstructions (see Supplemental Videos S1–S3). Morphology analysis was done under the criteria of elongated or round-shaped cells, and the percentage was calculated from panoramic immunofluorescence images of gels. On average, 75 cells were analyzed in each sample. Total degraded area from the fibrinolysis assay was quantified by the particle analysis tool using panoramic images (8×). Outlines of the degraded zones were drawn with the same software (see Supplemental Figure S3).

Statistical analysis

Statistical analyses were performed with GraphPad Prism 7 software (GraphPad Software, Inc., San Diego, CA, USA); data were obtained from quantifications of elongated and round-shaped cell proportions in fibrin hydrogels and of degraded areas. Intergroup analysis was carried out with two-way analysis of variance (ANOVA) followed by Tukey's test. The p values <0.05 were considered significant. Viability statistical analysis was done by one-way ANOVA followed by Tukey's test.

Results

Immunophenotype and mesodermal differentiation of PL-MSCs, BM-MSCs, and WJ-MSCs

Because there could be differences between MSCs sources, in the present study we compared MSCs from three different tissues: BM, PL, and WJ. They were characterized by analyzing the presence of markers associated with MSCs and by their capability to differentiate in mesodermal lineages. As was reported previously,[29] these cells showed high expression of CD105, CD90, CD73, and CD13; moderate to low expression of HLA-ABC; and low to absent expression of CD45, CD34, CD31, CD14, and HLA-DR (see Table 1, Figure 1(a)). PL-MSCs, BM-MSCs, and WJ-MSCs showed positive mesodermal differentiation, as confirmed by staining (see Figure 1(b)). For osteoblastic differentiation, cells were stained to detect alkaline phosphatase, while for chondroblastic differentiation, glycosaminoglycans were marked by their staining with Alcian blue; for adipoblastic differentiation, lipid droplets were stained with Oil Red O.

Viability of PL-MSCs, BM-MSCs, and WJ-MSCs in fibrin hydrogels

MSCs behavior in fibrin hydrogels was analyzed through viability, adhesion, and fibrinolysis assays. We used LIVE/DEAD staining to assay viability,[16,31] and found that MSCs from the three tissues were maintained viable after being cultured for up to 72 h in the hydrogel (>90%), at a similar rate as on 2D cultures on glass coverslips (~100%), as seen in Figure 2. In addition to viability, other aspects can be visualized in this assay. First, even though the morphology of cells grown on monolayer tends to be spindle-shaped, cells inside the fibrin hydrogel exhibited both round and elongated shapes. Second, PL-MSCs demonstrated a high fibrinolytic activity, as they degraded the fibrin hydrogel completely by the third to fourth day of culture and grew in monolayer on the plastic substrate (see Supplemental Figure S1). Both phenomena were evaluated in further detail.

FAs rich in vinculin and integrin αV are absent in PL-MSCs, BM-MSCs, and WJ-MSCs cultures in fibrin hydrogels

MSCs adhesion capability in 2D cultures and in fibrin hydrogels was evaluated by analyzing the presence of vinculin and integrin αV (FA proteins), and stress fiber formation. First, the presence of vinculin at FAs was analyzed after culturing MSCs on glass coverslips for 12, 24, 48, and 72 h, and in fibrin hydrogels for 0.5, 24, 48, and 72 h.

Monolayer conditions showed that cells were capable of adhering at 12 h, but spreading was clear at 24 h, along with stress fiber formation (see Figure 3). In every culture condition, vinculin was detected, and its presence in FAs increased as time in culture was augmented. Interestingly, in BM-MSCs, stress fibers appeared to be thicker and longer, and FAs had stronger vinculin detection, in comparison to PL-MSCs and WJ-MSCs, at all times.

As expected, MSCs adhesion in fibrin hydrogels was different with respect to the one observed in 2D cultures. From the first day, MSCs from the three tissues exhibited two shapes: round or elongated, but both with F-actin (see

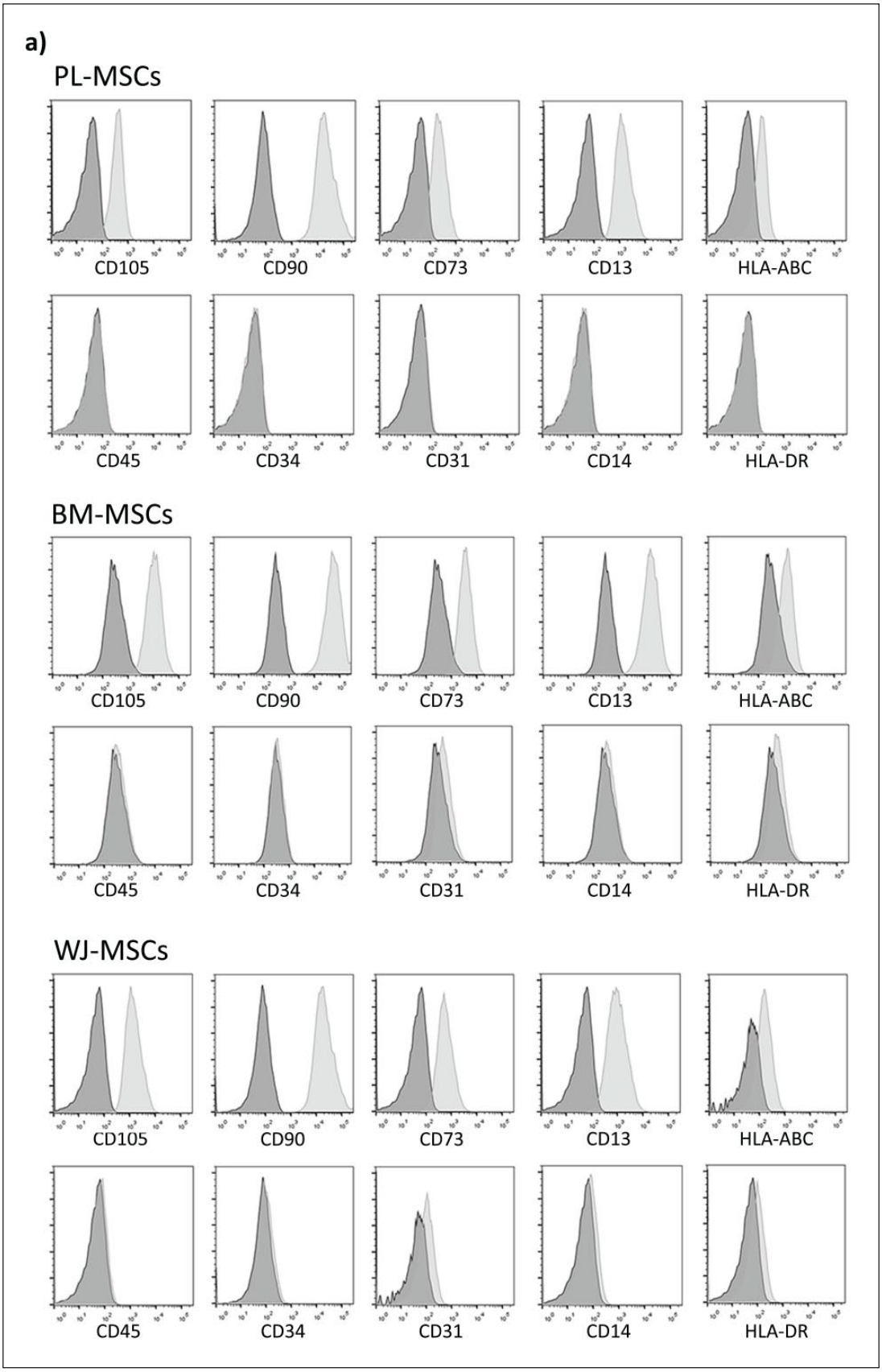
a)
PL-MSCs
CD105
CD90
CD73
CD13
HLA-ABC
CD45
CD34
CD31
CD14
HLA-DR
BM-MSCs
CD105
CD90
CD73
CD13
HLA-ABC
CD45
CD34
CD31
CD14
HLA-DR
WJ-MSCs
CD105
CD90
CD73
CD13
HLA-ABC
CD45
CD34
CD31
CD14
HLA-DR

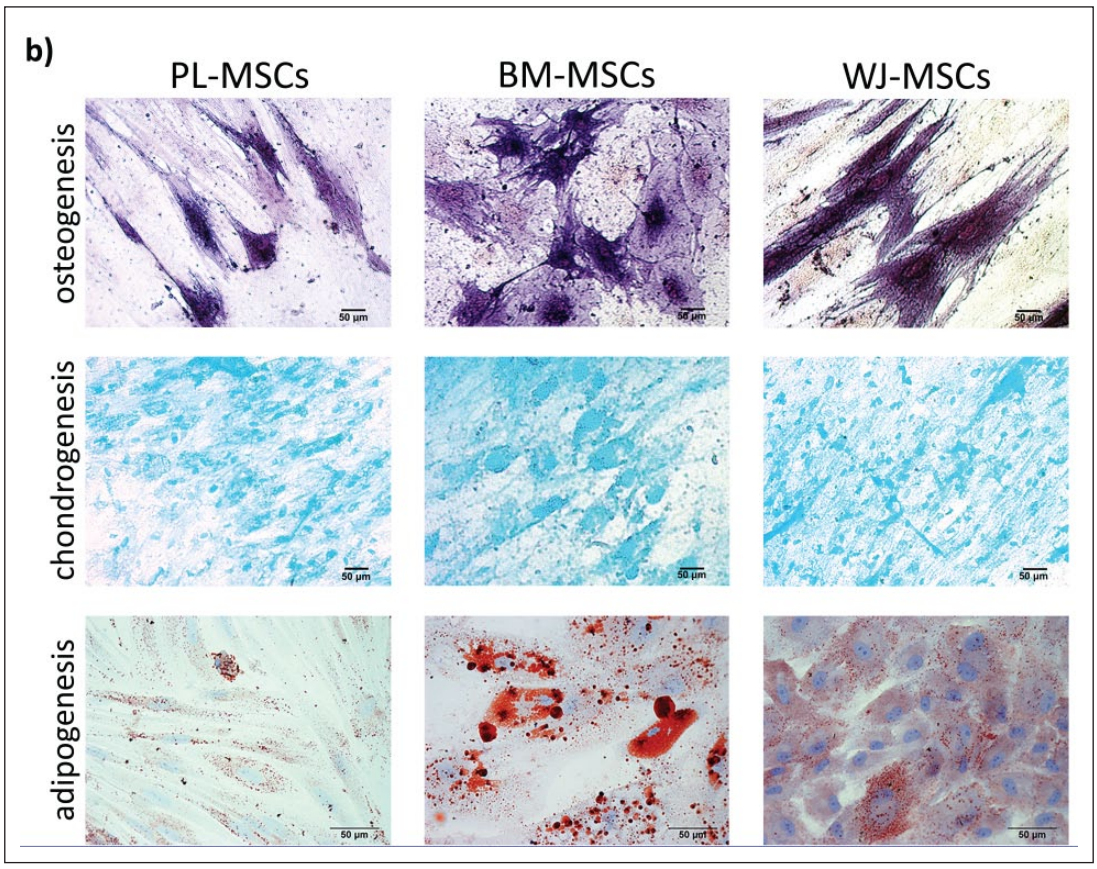

Figure 1. Immunophenotype and differentiation to mesodermal lineages of MSCs. (a) Cells were incubated with labeled antibodies for CD105, CD90, CD73, CD13, HLA-ABC, CD45, CD34, CD31, CD13, and HLA-DR, and analyzed by flow cytometry. Control (dark gray histograms) and positive populations (light gray histograms) are shown. (b) Osteoblastic differentiation was confirmed by alkaline phosphatase staining; glycosaminoglycans in chondroblastic differentiation were stained with Alcian blue, and lipid droplets in adipoblastic differentiation were stained with Oil Red O. Representative experiment. PL-MSCs: placenta mesenchymal stem cells; BM-MSCs: bone marrow mesenchymal stem cells; WJ-MSCs: Wharton's jelly mesenchymal stem cells.

Table 1. Immunophenotype of PL-MSCs, BM-MSCs, and WJ-MSCs.

Marker	PL-MSCs (% ±SD)	BM-MSCs (% ±SD)	WJ-MSCs (% ±SD)
CD105	96 ± 3	90 ± 13	99.8 ± 0.1
CD90	72.7 ± 27	85 ± 15	100
CD73	88 ± 9	97 ± 3	95.5 ± 6.6
CD13	98 ± 3	98 ± 1	97.8 ± 2.7
HLA-ABC	68 ± 30	94 ± 9	56.6 ± 32.1
CD45	2 ± 3	1 ± 1	0.1 ± 0.1
CD34	0	0	0.9 ± 0.8
CD31	1 ± 1	1 ± 1	6.6 ± 6.3
CD14	1 ± 1	2 ± 2	0.4 ± 0.3
HLA-DR	1 ± 1	3 ± 3	3.6 ± 4.9

PL-MSCs: placenta mesenchymal stem cells; BM-MSCs: bone marrow mesenchymal stem cells; WJ-MSCs: Wharton's jelly mesenchymal stem cells; SD: standard deviation.
The results are expressed as percentage of positive cells. SD of three experiments, with at least >10,000 events per sample, was counted (n = 3).

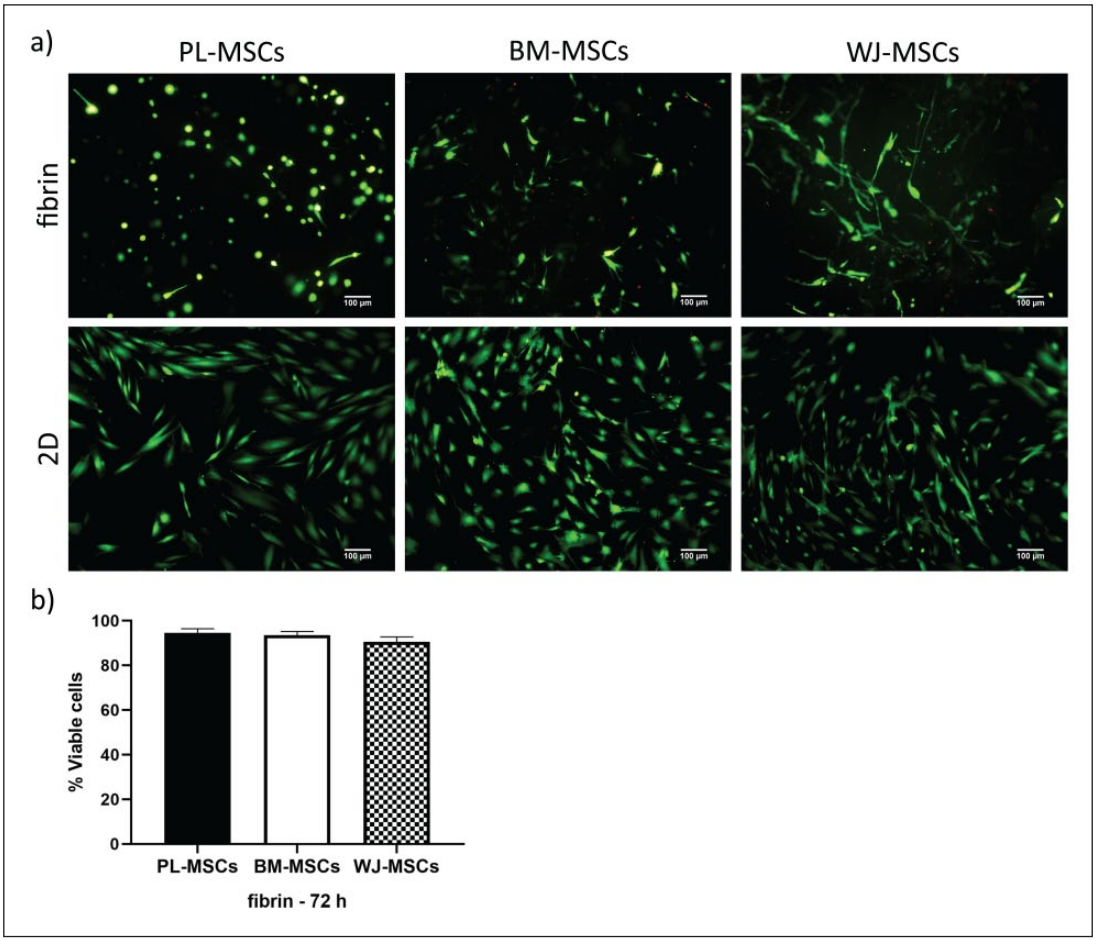

Figure 2. Viability of MSCs cultured in fibrin hydrogels and 2D. (a) Cells were stained with LIVE/DEAD kits; viable cells are seen in green, and dead ones in red. MSCs from different tissues showed a viability >90% at 3 days of culture in fibrin and almost 100% as a monolayer on glass coverslips. Images from a representative experiment were taken with an epifluorescence microscope. (b) Graph showing the percentages of viable cells in fibrin hydrogels at 3 days of culture. Bars indicate standard errors of the media of three experiments. There were no statistical differences between MSCs ($p < 0.05$) ($n = 3$). PL-MSCs: placenta mesenchymal stem cells; BM-MSCs: bone marrow mesenchymal stem cells; WJ-MSCs: Wharton's jelly mesenchymal stem cells.

Figure 4(a)). These morphologies were more evident at 48 h, and their proportions were different between the three types of MSCs. After culturing for 2 days, $91.12 \pm 1.92\%$ of PL-MSCs were round-shaped cells, which represent approximately 2-fold and 1.2-fold greater than in BM-MSCs and WJ-MSCs ($44.44\% \pm 7.74\%$ and $76.84\% \pm 0.01\%$), respectively, with statistically significant difference in comparison to BM-MSCs ($p = 0.0007$) (see Figure 4(b)). We observed that elongated cells from MSCs of the three sources were less widespread in fibrin hydrogels than those seeded on glass coverslips; nonetheless, BM-MSCs tended to be more ramified in fibrin hydrogels than the other two. Despite the differences between elongated and round-shaped cells in the three sources of MSCs, they were positive for CD105 regardless of their morphology and/or expression of the other markers, as shown for WJ-MSCs in Figure 5(c). In one instance, elongated cells in BM-MSCs and WJ-MSCs developed thicker stress fibers than in PL-MSCs, although vinculin seems not to be present in them (see Figure 4(a)). In another instance, round-shaped cells from the three sources of MSCs had F-actin in aggregates with the submembranous location of vinculin, and only some PL-MSCs contained lamellipodia with low to absent vinculin detection (see Figures 4(a) and 5(b), and Supplemental Videos S1–S3). Moreover, vinculin was detected in round-shaped cells, with increased intensity as time in culture was augmented and was partially colocalized with actin, although there were no apparent FAs. PL-MSCs completely degraded the fibrin hydrogel between the third and fourth day of culture (see Supplemental Figure S1(a)), dropping to the bottom of the tissue culture plate and generating a monolayer. These cells were stained to evaluate vinculin and actin, showing they were still capable of displaying stress fibers and FAs in 2D cultures (see Supplemental Figure S1(b)).

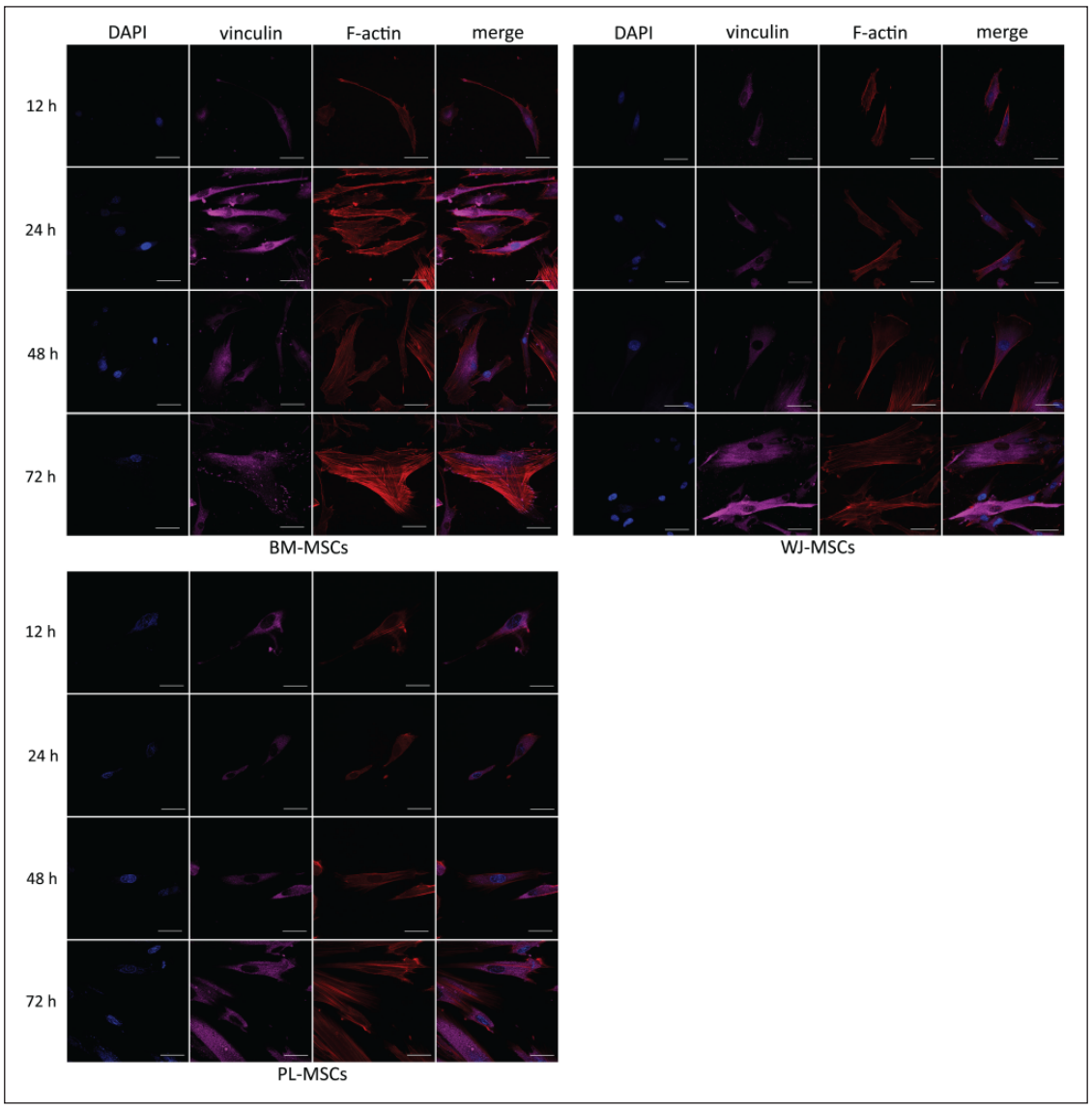

Figure 3. Temporal course of vinculin and actin distribution in MSCs cultured on 2D. Cells were cultured on glass coverslips for 12 h, 1, 2, and 3 days, fixed and stained for nuclei (blue), F-actin (red), and vinculin (magenta). In each case, vinculin detection in FAs was augmented in a time-dependent manner. Representative confocal micrographs are shown. PL-MSCs: placenta mesenchymal stem cells; BM-MSCs: bone marrow mesenchymal stem cells; WJ-MSCs: Wharton's jelly mesenchymal stem cells. Bars represent 50 μm.

Later, we evaluated integrin αV in MSCs cultured in monolayer as well as in fibrin hydrogels for 2 days. As shown in Figure 5(a), MSCs cultures in 2D expressed integrin αV in FAs, where it colocalized with vinculin and actin. In fibrin hydrogels, integrin αV was found in some elongated and round-shaped cells of PL-MSCs and BM-MSCs, but its detection was null in almost all cells in WJ-MSCs cultures (see Figure 5(b); Supplemental Figure S2 and Videos S1–S3). In all cases, detection of integrin αV in FAs was weak. As previously mentioned, only some round-shaped PL-MSCs had lamellipodia, with a diffuse staining of vinculin and integrin αV at 2 days (see Figure 5(b) and Supplemental Video S1).

Fibrin hydrogels were degraded by PL-MSCs, BM-MSCs, and WJ-MSCs at different rates

We evaluated the fibrinolytic activity of MSCs from the three tissues cultured in fibrin hydrogels in the presence and absence of inhibitors of the plasminogen–plasmin axis and MMPs. Cells were cultured for 7 days in a very low cell number (1500 cells/mL) in the presence or absence of aprotinin, tranexamic acid, BB-94, and their combinations, after which degradation analysis was carried out (see Figure 6(b) and (c)). With the use of image analysis software, degraded zones per hydrogel were selected and numbered, and their areas were calculated as described in

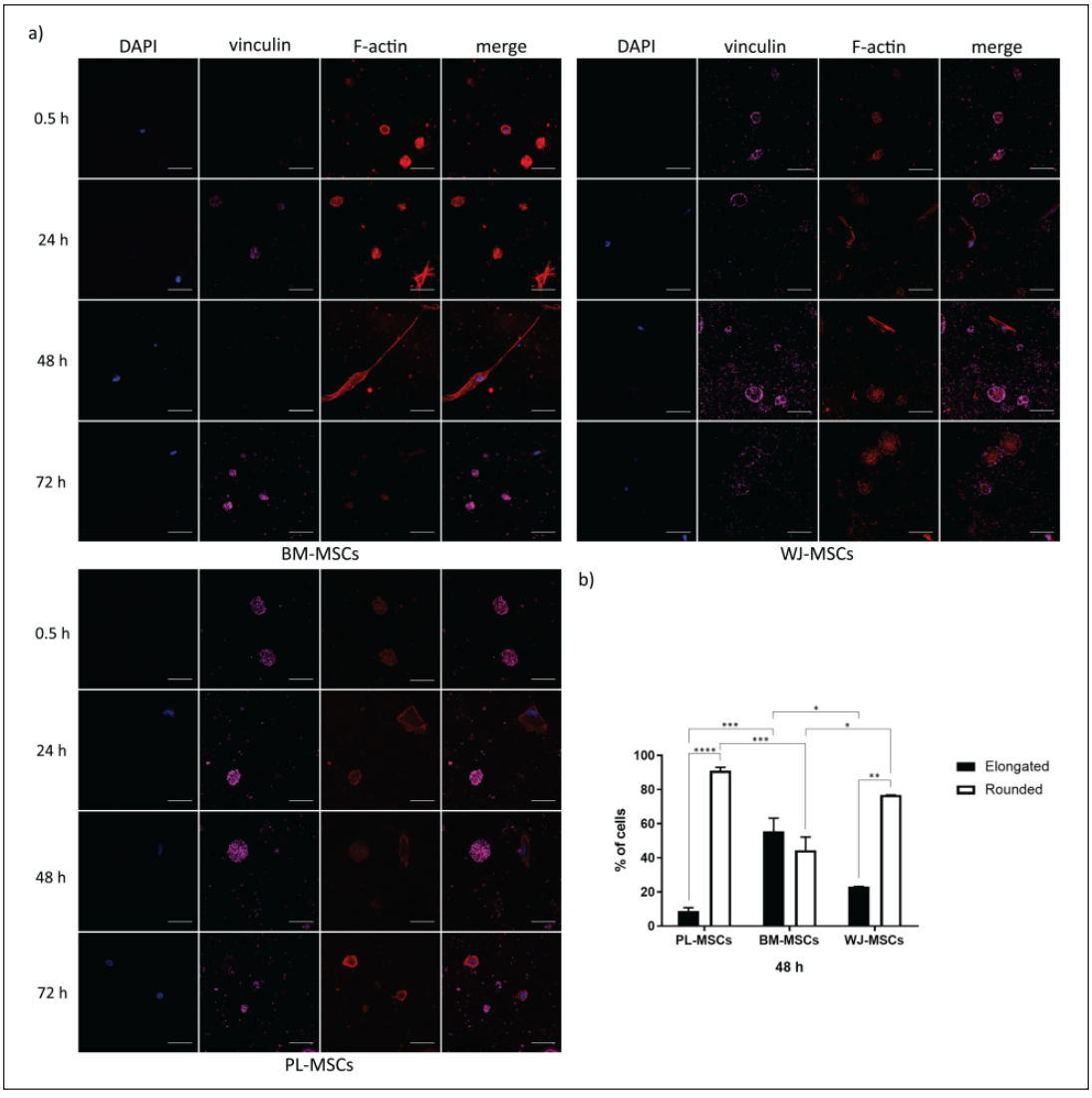

Figure 4. Temporal course of vinculin and actin distribution in MSCs cultured in fibrin hydrogels. (a) Cells were cultured in fibrin hydrogels for 0.5 h, 1, 2, and 3 days, fixed and stained for nuclei (blue), F-actin (red), and vinculin (magenta). In each case, two phenotypes can be observed: round-shaped cells positive for vinculin, and elongated cells negative for the marker. Representative confocal micrographs are shown. Bars represent 50 μm. (b) Graph showing the percentages of elongated and round-shaped cells in MSCs cultured in fibrin hydrogels for 2 days. Bars indicate standard errors of the media of three experiments, and 75 cells on average per sample were counted (n = 3). *p = 0.0204, **p = 0.0011, ***p = 0.0007, and ****p < 0.0001. PL-MSCs: placenta mesenchymal stem cells; BM-MSCs: bone marrow mesenchymal stem cells; WJ-MSCs: Wharton's jelly mesenchymal stem cells.

the "Materials and methods" section (see Supplemental Figure S3). The percentages of total degraded areas are shown in Figure 6(c).

In 2-day cultures and in the absence of inhibitors, MSCs from the three tissues were capable of generating lytic zones, which at 7 days reflected different lytic rates (see Figure 6(a)–(c)). Without inhibitors, PL-MSCs almost completely degraded the hydrogel (90.81% ± 1.88%), leaving only traces, whereas BM-MSCs and WJ-MSCs generated limited lysis (BM-MSCs, 17.72% ± 0.67%; WJ-MSCs, 22.1% ± 2.58%), and these differences were significant (see Figure 6(b) and (c)). The high degradation generated in hydrogels seeded with PL-MSCs could not be diminished by BB-94, as the degraded area was approximately 88.04% ± 0.97%, while tranexamic acid and aprotinin decreased it two- and sixfold, respectively (TA: 58.98% ± 6.79%; Ap: 16.19% ± 0.33%) (see Figure 6(c)). Thus, aprotinin was the most efficient inhibitor and BB-94 the least. These observations were repeated with hydrogels seeded with WJ-MSCs and BM-MSCs, although the differences compared with hydrogels without inhibitors were not significant. Among the three combinations of inhibitors used, the one with the strongest effect was aprotinin/tranexamic acid (PL-MSCs, 8.69% ± 2.19%; BM-MSCs, 7.81% ± 0.47%; WJ-MSCs, 14.44% ± 1.85%).

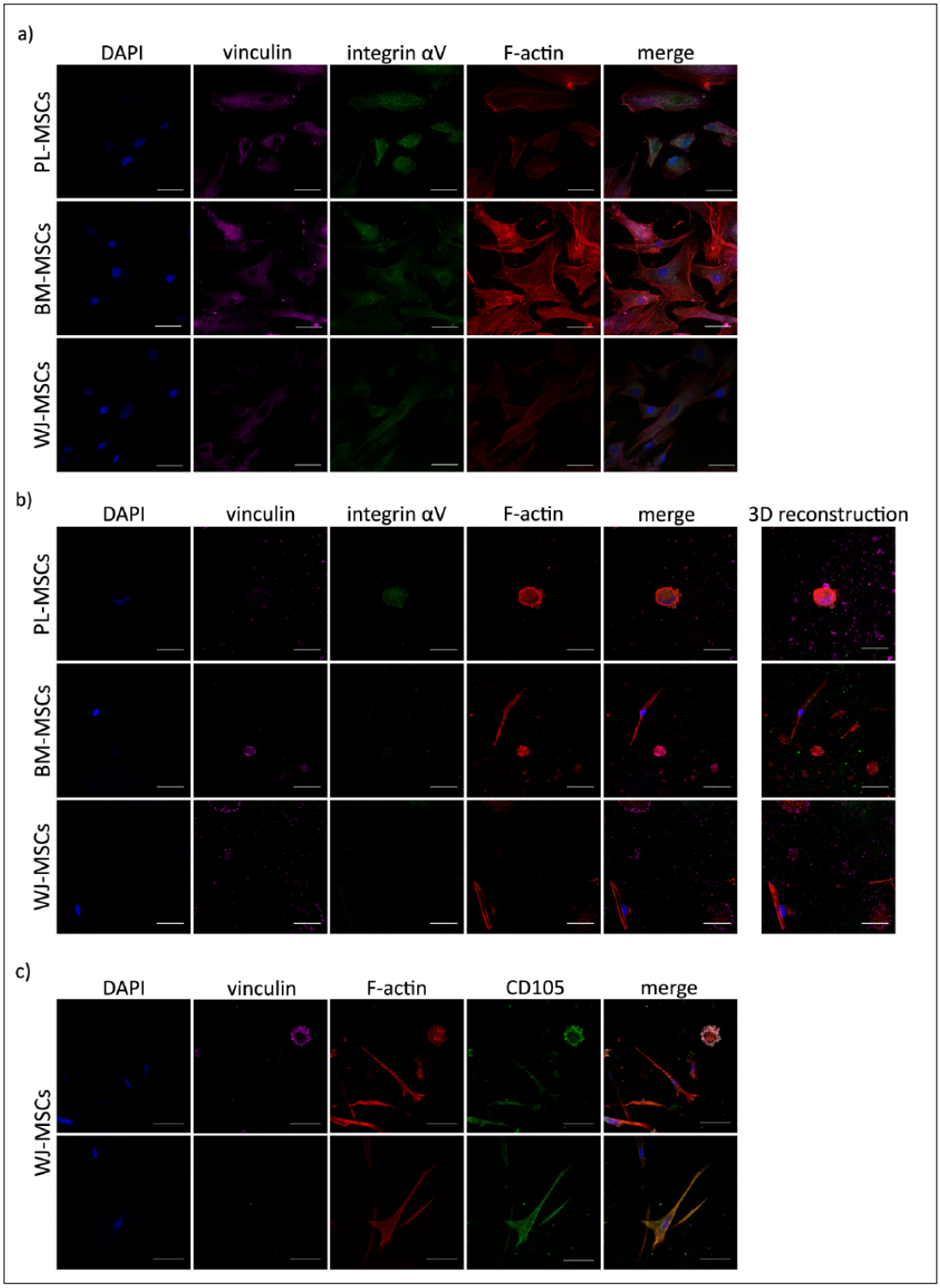

Figure 5. Presence of integrin αV in MSCs cultured in 3D fibrin hydrogel and 2D. (a) Integrin αV detection in MSCs cultured as monolayer on glass coverslips for 48 h. Cells were fixed and stained for nuclei (blue), actin (red), vinculin (magenta), and integrin αV (green). In each case, integrin αV was detected in FAs, where it partially colocalized with F-actin and vinculin. (b) Integrin αV detection in MSCs cultured in fibrin hydrogels for 48 h. Cells were fixed and stained for nuclei (blue), actin (red), vinculin (magenta), and integrin αV (green). Integrin αV was detected in some elongated and round-shaped cells; 3D reconstructions are displayed (see Supplemental Videos S1–S3). (c) CD105 marker in WJ-MSCs cultured in fibrin. Cells were fixed and stained for nuclei (blue), actin (red), vinculin (magenta), and CD105 (green). CD105 was detected in elongated and round-shaped cells. This was also observed in PL-MSCs and BM-MSCs (data not shown). (a)–(c), representative confocal micrographs are shown. PL-MSCs: placenta mesenchymal stem cells; BM-MSCs: bone marrow mesenchymal stem cells; WJ-MSCs, Wharton's jelly mesenchymal stem cells. Bars represent 50 μm.

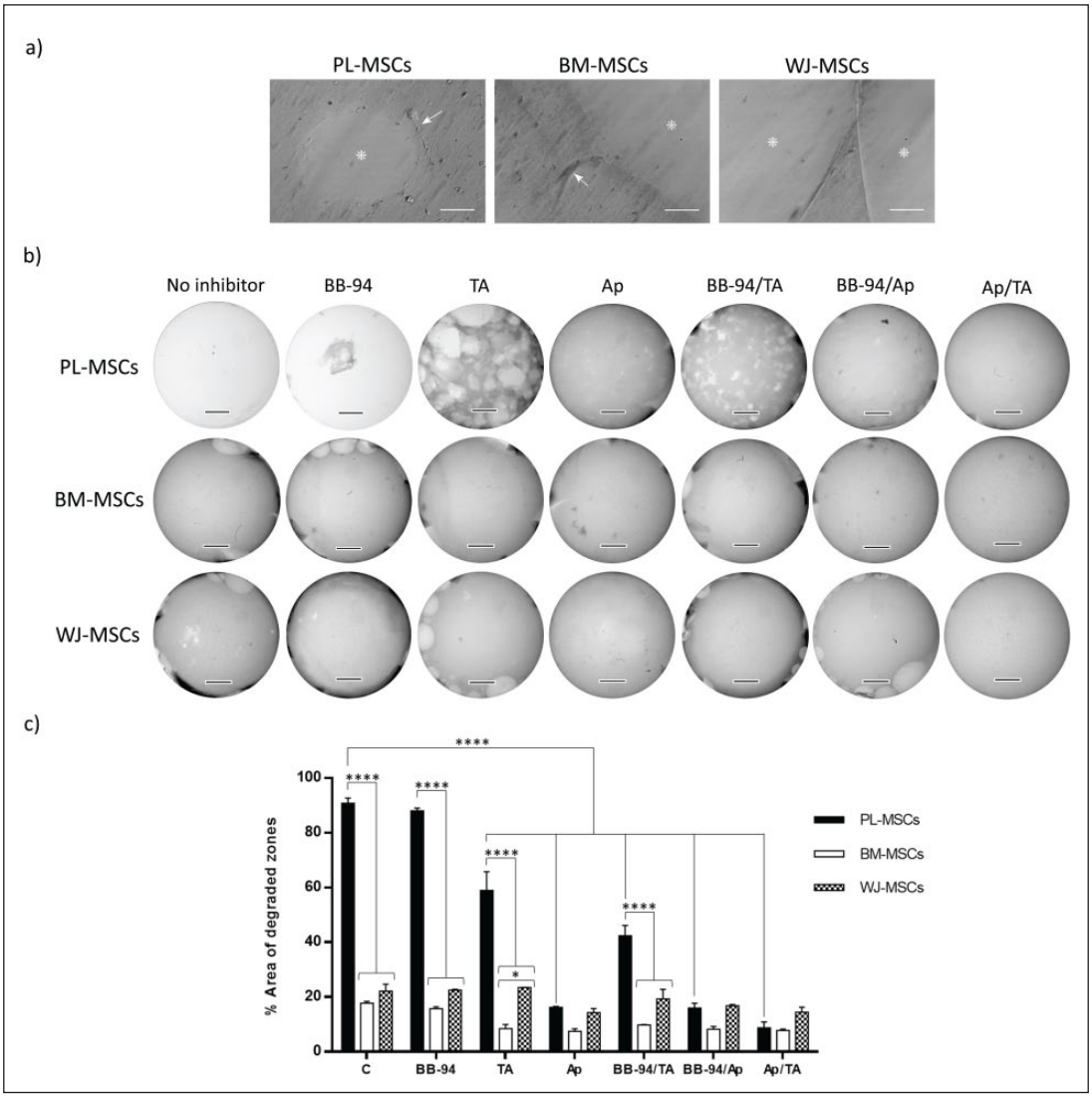

Figure 6. Fibrinolysis by MSCs. (a) Cells seeded in fibrin gels generated hydrolysis at 48 h of culture. Images show degraded zones (*) and cells (arrows). Bars represent 50 μm. (b) Cells seeded in fibrin gels in the presence or absence of inhibitors—Ap (200 μg/mL), TA (400 μg/mL), BB-94 (5 μM), and their combinations—generated distinct levels of hydrolysis at 7 days of culture. Bars represent 3 mm. (c) Semi-quantification of total area of degraded zones done by MSCs in the presence or absence of inhibitors. Bars indicate standard errors of two experiments (n = 2). *p = 0.0104 and ****p < 0.0001. PL-MSCs: placenta mesenchymal stem cells; BM-MSCs: bone marrow mesenchymal stem cells; WJ-MSCs: Wharton's jelly mesenchymal stem cells; TA: tranexamic acid; Ap: aprotinin.

Discussion

In 2006, the ISCT established the minimal criteria for MSCs identity, principally for BM-MSCs.[9] However, in the last few years, new tissue sources and characteristics have emerged for MSCs. MSCs have been isolated from PL, umbilical cord, AT, and dental pulp. Although research in tissue engineering and regenerative medicine has mainly been performed with BM-MSCs, as they continue to be the gold standard, there is a high potential to consider other sources because of the accessibility for their isolation.

As others have stated, MSCs isolated from various tissues may behave differently in certain contexts,[10,28,32] and this is important if they are intended to be used for cellular therapy. The aim of this work was to understand the biology of the MSCs by comparing the viability, adhesion, and fibrinolytic activities of PL-MSCs, BM-MSCs, and WJ-MSCs cultured in fibrin hydrogels from nonpurified plasma. Our results shed a light on MSCs behavior in a physiological microenvironment, and this is the first time that the adhesion and fibrinolytic activity of MSCs isolated from different tissues are compared in fibrin hydrogels generated from nonpurified plasma.

BM-MSCs, WJ-MSCs, and PL-MSCs used in this study shared the expected immunophenotype and the capability to differentiate in vitro to mesodermal lineages, as well as to adhere to plastic tissue culture (see Table 1 and Figure 1).

Moreover, viability assays in 2D (on glass coverslips) and in 3D (fibrin hydrogels) with LIVE/DEAD staining showed that MSCs isolated from the three tissues were viable in both contexts at similar rates (>90%) (see Figure 2). As noted previously, two other phenomena were revealed with this assay: the different cellular morphologies in fibrin hydrogels and the greater degradation capability of PL-MSCs than MSCs from BM and WJ. LIVE/DEAD staining has been used in the past as an indirect method to evaluate adhesion and proliferation, as cell elongation is necessary for both cell activities. Ho et al.[16] observed that BM-MSCs morphology and proliferation in fibrin hydrogels (prepared with purified fibrinogen) were dependent on fibrinogen concentration. BM-MSCs cultured in fibrin hydrogels prepared with 5 mg/mL of fibrinogen were spindle-shaped and proliferating, while those seeded in 50 mg/mL gels stayed rounded and nonproliferating, even after 12 days of culture. Although our fibrin hydrogels have 2.925 ± 0.15 mg/mL of fibrinogen (prepared with nonpurified plasma), most of the PL-MSCs had round shape, while a mixed population of elongated and round-shaped cells was found in BM-MSCs and WJ-MSCs. The different behavior of the cells reveals the potential clinical relevance of the sources used, being necessary to be considered for future studies. Moreover, we explored cell adhesion by analyzing the presence of two FA proteins, vinculin and integrin αV, in 2D and 3D contexts. PL-MSCs, WJ-MSCs, and BM-MSCs cultured in 2D had vinculin in FAs, and this detection increased with time in culture (see Figure 3). Focal complexes, FAs, fibrillar adhesions, and 3D matrix adhesions are multiprotein structures mediating cell–ECM interactions.[33] In 2D cultures, FAs connect the actin cytoskeleton to ECM through integrins, and it has been stated that substrate rigidity alters the molecules involved. Vinculin is a mechanosensory protein that is activated by a rigid substrate and then recruited to FAs.[34] Van Tam et al.[35] demonstrated that BM-MSCs exhibited FAs rich in vinculin, talin, and paxillin when seeded on a substrate made of polycaprolactone with rigidity ranging from 0.9 to 133 MPa, but not in Matrigel, a soft substrate. Here, PL-MSCs, BM-MSCs, and WJ-MSCs had a similar capability to form vinculin-positive FAs in 2D cultures.

In every case, MSCs cultured in fibrin hydrogels exhibited two phenotypes. In the first phenotype, cells showed an elongated morphology with stress fibers (BM-MSCs and WJ-MSCs) or with a disorganized actin cytoskeleton (PL-MSCs), without detection of vinculin (see Figure 4). In the second phenotype, the morphology was rounded, with aggregates of F-actin, as phalloidin staining only marks actin filaments, and vinculin showed a diffuse distribution, but only PL-MSCs had lamellipodia (see Figures 4(a) and 5(b), and Supplemental Videos S1–S3). Vinculin presence in FAs has been questioned in the past due to a low or null detection in soft scaffolds, such as collagen hydrogels or Matrigel.[22],[35] Van Tam et al.[35] found that BM-MSCs seeded on Matrigel were able to spread and migrate inside it, but cells did not have vinculin, talin, nor paxillin. In addition, vinculin null detection in elongated cells may be explained by a lack of rigidity in the substrate, as poor mechanical strength for whole fibrin hydrogels from purified fibrinogen (<1 kPa) has been reported.[36] Our results contrast with the ones reported by Hakkinen et al.,[24] who observed vinculin-positive FAs in fibroblasts cultured in fibrin hydrogels (purified fibrinogen) and other matrices. It should be mentioned that the dermal fibroblasts they used might behave differently from MSCs in the same microenvironment, and the fibrin hydrogels they used and ours represent two distinct scaffolds. Fibers from hydrogels prepared with nonpurified plasma have thicker and softer fibers than those from purified fibrinogen.[37] In our system, fibrin hydrogel rigidity depends not only on its origin (nonpurified plasma) but also on fibrinolysis carried out by MSCs, especially by PL-MSCs, which will be discussed later. It must be considered that vinculin null detection does not rule out the existence of FAs, as other proteins such as paxillin and talin may be present, which needs further investigation.

Round-shaped cells found in our system have been reported for undifferentiated MSCs. Ho et al.[16] published that BM-MSCs cultured in fibrin hydrogels prepared with a high purified fibrinogen concentration adopted a rounded morphology, but they did not assess FA protein presence. However, MSC cytoskeletal instability has been associated with adipogenesis and chondrogenesis.[25],[38],[39] In respect to chondrogenesis, it has been reported that BM-MSCs cultured for 7 days in agarose hydrogels in the presence of an inductor media showed a rounded morphology and diffuse marks for vinculin, actin, vimentin, and tubulin proteins.[40] Because agarose lacks arginine–glycine–aspartic acid (RGD) sites, the authors claim that MSCs cannot adhere to it, so they do not spread and generate their pericellular matrix, rich in collagen and proteoglycans. Moreover, BM-MSCs chondrogenesis in agarose hydrogels has been inhibited through RGD–integrin adhesion dependent on cytoskeletal organization.[41] The round-shaped cells we found could be later used for chondrogenic differentiation under adequate chemical stimulus, as plasma carries many growth factors that may induce the overexpression of chondrogenic markers, which should be investigated further. Considering that PL-MSCs also presented round-shaped cells that do not match the previous phenotype (lamellipodia formation), the MSCs source might be affecting how they interact with the fibrin hydrogel. In fact, only PL-MSCs completely degraded the hydrogel and formed a monolayer on the tissue culture capable of adhering through FAs (see Supplemental Figure S1).

Because our hydrogel has RGD sites, the behavior of the cells might be related to recognition by integrins. RGD clustering in hyaluronic acid hydrogels induced cell spreading and modulation of integrin expression in mouse

MSCs.[42] Various integrins recognize RGD sites, such as αVβ3, αVβ5, αVβ6, αVβ8, α5β1, and α11bβ3, although αVβ3 has the best affinity.[43] In 2D cultures, MSCs from the three different sources had the ability to form FAs in which integrin αV colocalized with vinculin and actin (see Figure 5(a)). In contrast, in hydrogels, integrin αV was only found in some elongated and round-shaped cells in cultures from BM-MSCs and PL-MSCs, but was low to null in elongated cells from WJ-MSCs, even though FAs were absent (see Figure 5(b), Supplemental Figure S2, and Supplemental Videos S1–S3). Apparently, integrin αV is unnecessary for MSCs adhesion to fibrin hydrogel; however, other integrins may have a role or cells might interact with the scaffold through another adhesion mechanism, such as recognition of haptides.[44] Khetan et al.[25] demonstrated that hyaluronic acid hydrogel degradation by BM-MSCs was necessary for them to adhere, generate traction forces, and differentiate toward an osteogenic phenotype. As the percentages of elongated and round-shaped cells varied among MSCs, this may reflect the kind of activity they are developing in the hydrogel. It can be suggested that some cells seeded in fibrin hydrogels can adhere, generate traction forces, and spread, while those who cannot stay rounded, even though they would interact with the scaffold. It has been reported that MSC seeded in scaffolds, consisting of fibers, must adhere to, pull, and remodel fibers in order to spread.[45,46] Moreover, BM-MSCs and WJ-MSCs degradation rates are minimum, allowing some cells to attach and elongate. On the other hand, high fibrinolysis generated by PL-MSCs loosens the hydrogel, limiting the attaching sites, which may cause an impaired spreading and the maintenance of the round shape of the cells.

In vivo, fibrinogen polymerization is a biological process consequence of hemostasia, and fibrinolysis is the counterpart occurring after the blood clot is no longer needed. The principal fibrinolytic enzyme is plasmin, which happens to be a zymogen found in plasma activated by uPA and tPA.[14,47] Fibrin hydrogel polymerization appears to represent the last part of the coagulation cascade. Fibrin hydrogel degradation by MSCs has been reported for BM-MSCs, but not for WJ-MSCs and PL-MSCs.[26,27,48] Blood plasma carries many proteins, such as coagulation factors, complement proteins, cytokines, lipoproteins, albumin, hemoglobin, fibronectin, and growth factors, as platelet-derived growth factor (PDGF).[49,50] In contrast to hydrogels prepared with purified fibrinogen, nonpurified plasma may bring along many of these proteins. Although it is not known which growth factors or cytokines induce the phenotypes observed, PDGF may have a role in fibrinolysis. It has been reported that therapeutically noneffective AT-MSCs from diabetic patients presented diminished proliferation, migration, homing to the wound bed, and an overall increased profibrotic phenotype, all rescued with the exposure to PDGF-two B subunits (PDGF-BB).[51] Specifically, PDGF-BB increased fibrinolytic activity of AT-MSCs from donors and diabetic patients, although diabetic cells were less sensitive to the treatment.[51] However, this must be confirmed in MSCs isolated from other tissues, like those used in this work.

Here, we evaluated MSCs fibrinolytic activity after culturing them for 7 days in fibrin hydrogels in the absence or presence of the inhibitors BB-94, aprotinin, tranexamic acid, and their combinations. Later, total degraded areas were quantified by software. It must be considered that this evaluation gives us limited quantification for two reasons. First, the images were taken at 8×, so the software may be depreciating the smallest degraded zones. Second, it does not consider the gel volume. Nonetheless, it offers an idea of the observed lysis. As shown in Figure 6(a), lysis can be appreciated as holes (BM-MSCs in the presence of BB-94) and cavities (WJ-MSCs in the presence of BB-94), which may be a result of the differential presence and activity of the fibrinolytic enzymes and their regulators involved. Our results showed that MSCs from different sources hydrolyzed fibrin at different rates and that this activity was best inhibited by the combination of aprotinin–tranexamic acid in every case (see Figure 6).

BB-94 is a general metalloprotease inhibitor, and the other two inhibit the plasminogen–plasmin axis. Tranexamic acid is a lysin analog that joins the binding sites of plasminogen/plasmin to fibrin, while aprotinin inhibits plasmin and other serine proteases. Considering that BM-MSCs were reported to not express plasmin,[27] it was possible that MSCs secreted other fibrinolytic enzymes. Thus, as others have stated, these enzymes include metalloproteases MMP-1, MMP-2, MMP-3, MMP-7, MMP-9, MMP-11, MMP-13, MT1-MMP, MT2-MMP, and MT3-MMP,[52] which are expressed by BM-MSCs, traumatized muscle MSCs (TM-MSCs), and AT-MSCs.[53] As BB-94 was the least inhibitor of MSCs fibrinolysis, it can be suggested that MMPs have little or no effect and that the plasminogen–plasmin axis principally accounts for it. Considering that aprotinin decreased fibrinolysis more than tranexamic acid, the participation of other enzymes aside from plasmin cannot be ruled out. According to Neuss et al.,[27] BM-MSCs hydrolyze fibrin gels (from purified fibrinogen) twofold compared with dermal fibroblasts, and they express uPA, tPA, PAI-1, and uPAR. It has been reported that a high basal expression of PAI-1 and a low expression of cathepsins B and D by WJ-MSCs decreased their capability to migrate through Matrigel, which is opposite to BM-MSCs and PL-MSCs.[28] Although fibrin hydrogel composition differs from Matrigel, PAI-1 expression was directly responsible for diminished MSCs migration capability, which is indirectly related to lower hydrogel degradation. In this work, the differential rate of fibrinolysis by distinct types of MSCs could be a consequence of differential regulation of the plasminogen–plasmin axis and the expression of other fibrinolytic enzymes, such as cathepsins B and D, which should be further investigated.

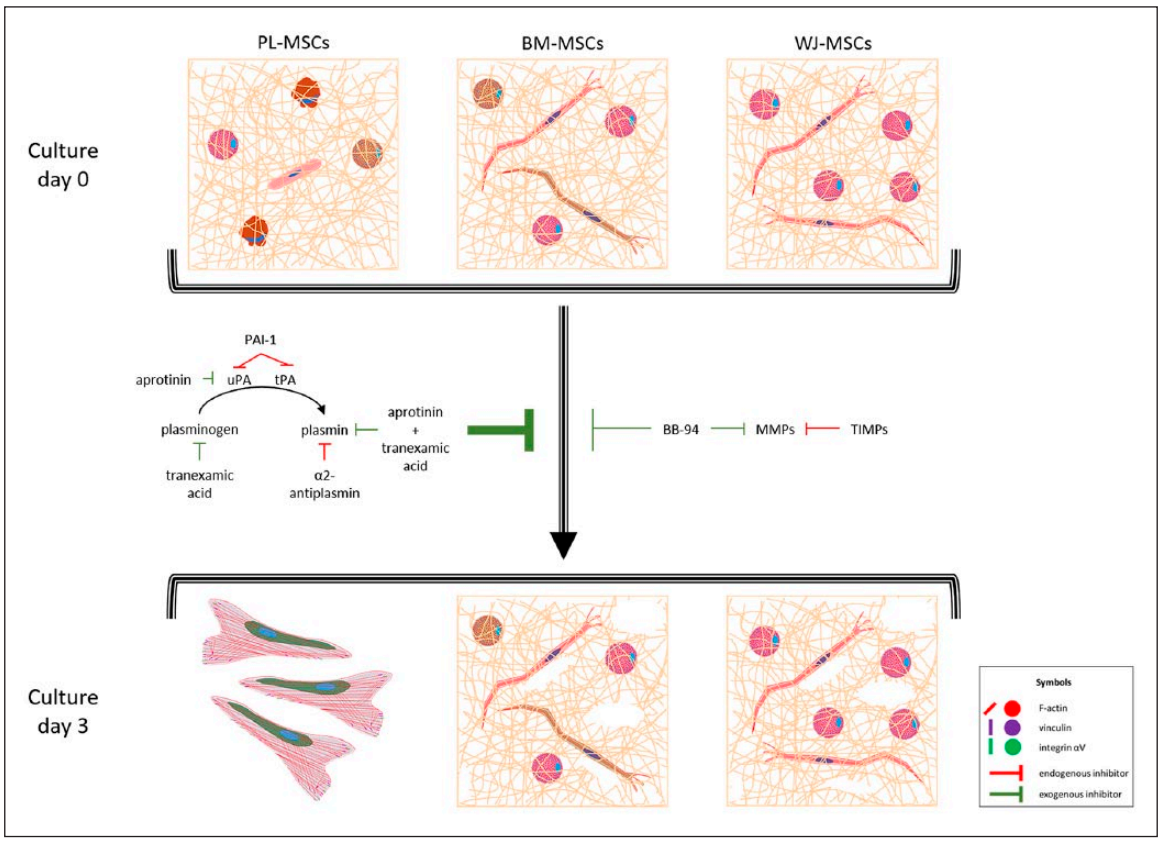

Figure 7. MSCs adhesion to fibrin hydrogels and fibrinolysis effect. MSCs from the three tissues cultured in fibrin hydrogels exhibited elongated and round phenotypes, with actin in filaments or aggregates, respectively. Vinculin and integrin αV were not necessary for adhesion, as they were absent in FAs, and only some cells were positive for both proteins. Proportions of elongated and round-shaped cells varied between the three types of MSCs accordingly to their capabilities to degrade fibrin hydrogel. PL-MSCs were rounded in >90%, degraded the hydrogel completely, and generated a monolayer with FAs rich in vinculin (see Supplemental Figure S1), and were positive probably for integrin αV (as it was shown in 2D cultures, see Figure 5). BM-MSCs and WJ-MSCs degraded fibrin in a limited way, and after 3 days they still gathered inside it. In all cases, aprotinin and tranexamic inhibited fibrinolysis more than BB-94, meaning that it was done principally via the plasminogen–plasmin axis. uPA: urokinase plasminogen activator; tPA: tissue plasminogen activator; PAI-1: plasminogen activator inhibitor 1; MMPs: metalloproteases; TIMPs: tissue inhibitors of metalloproteases.

Although it is not known why MSCs from distinct tissues cultured in fibrin hydrogels show different morphologies, adhesion, and fibrinolytic rates, those activities might be related. To survive, MSCs need to adhere to a substrate, and its rigidity will determine the adhesion strength. Fibrin hydrogel is a soft substrate that cannot support a strong adhesion, although it allows for some cells to adhere and spread. In the case of PL-MSCs, elongated cells were in a very low percentage and possessed a disorganized cytoskeleton, meaning that fibrinolysis affected substrate mechanical properties. This might have therapeutic significances. For instance, round-shaped cells with cytoskeleton instability and no lamellipodia had a similar phenotype to MSCs observed in chondrogenesis,[18,40] and these were more prevalent in WJ-MSCs. In another, BM-MSCs deficient in fibrinolysis remodeling (MSCs PTX3$^{-/-}$) presented a diminished implantation in cutaneous wound beds, and therefore a delay in wound healing.[48] In addition, some diabetic patients developed distal microthrombosis after an autologous transplantation of AT-MSCs, which is related to a low fibrinolytic activity in vitro compared to nondiabetic cells.[54] Because PL-MSCs degraded the most, they may be good candidates for wound healing therapy. On the other hand, it must be considered that in vivo WJ-MSCs are embedded in a connective fetal tissue surrounding and protecting umbilical cord vessels, while BM and PL-MSCs support hematopoiesis and vasculogenesis.[55] The differences in their physiological roles may be related with their behavior in our work; however, their participation in thrombosis or fibrinolysis in vivo has not been studied.[56,57]

Taken together, our results showed that PL-MSCs, BM-MSCs, and WJ-MSCs shared the characteristics established for MSCs identity; they formed FAs rich in vinculin and integrin αV in 2D; and they behaved differently when cultured in fibrin hydrogels from nonpurified plasma (see Figure 7), as shown by FA analysis. Cellular spreading was a vinculin independent phenomenon, and it is not clear if

vinculin is participating in rounded cell adhesion, even though they did not require the presence of integrin αV. Moreover, PL-MSCs degraded fibrin hydrogel more than BM-MSCs and WJ-MSCs. This is the first time that adhesion and fibrinolysis were compared for three different sources of MSCs, and the differences observed are remarkable. If the phenotypes displayed by MSCs in a natural environment do relate to specific behaviors that could be directed to cartilage and bone tissue engineering, or to chronic wound repair according to its source, this should be a theme for future works.

Conclusion

MSCs isolated from BM, PL, and WJ shared a similar immunophenotype, mesodermal differentiation capabilities, spindle-shape morphology, and FAs in 2D cultures, in contrast to their behaviors in fibrin hydrogels. There, MSCs did not form FAs rich in vinculin or integrin αV, exhibited different phenotypes, and were able to degrade fibrin hydrogels at different rates, principally through the plasminogen–plasmin axis. Our findings denote tissue-specific capabilities regarding the culture in a physiological microenvironment, which is necessary to take into consideration when different sources of MSCs are included for cellular therapy, tissue engineering, and regenerative medicine.

Acknowledgements

The authors would like to thank Marta Castro Manrreza for her knowledge of mesenchymal stem cells (MSCs), María José Gomora Herrera and José Alfredo Jimenez for their technical support in confocal microscopy, and Katia Jarquín Yáñez and Sara Judith Alvarez Pérez for their technical support.

Declaration of conflicting interests

The author(s) declared no potential conflicts of interest with respect to the research, authorship, and/or publication of this article.

Funding

The author(s) disclosed receipt of the following financial support for the research, authorship, and/or publication of this article: The present study was conducted under the financial support of PAPIIT-DGAPA-UNAM (IN218315, IN108116, and IN22316). This article is a requisite for the obtainment of a PhD degree for MSc Casandra Paulina Chaires-Rosas, who received academic support from Biological Sciences Postgraduate program, UNAM, and financial support from CONACYT (263778). Dr Xóchitl Ambriz was supported by a postdoctoral scholarship from DGAPA-UNAM (2016–2018) and Faculty of Medicine (UNAM).

ORCID iDs

Javier R Ambrosio https://orcid.org/0000-0001-7441-0609
Andrés Castell-Rodríguez https://orcid.org/0000-0003-2881-2759

Supplemental material

Supplemental material for this article is available online.

References

1. Falanga V, Iwamoto S, Chartier M, et al. Autologous bone marrow-derived cultured mesenchymal stem cells delivered in a fibrin spray accelerate healing in murine and human cutaneous wounds. *Tissue Eng* 2007; 13(6): 1299–1312.
2. Liu L, Yu Y, Hou Y, et al. Human umbilical cord mesenchymal stem cells transplantation promotes cutaneous wound healing of severe burned rats. *PLoS ONE* 2014; 9(2): e88348.
3. Mehanna RA, Nabil I, Attia N, et al. The effect of bone marrow-derived mesenchymal stem cells and their conditioned media topically delivered in fibrin glue on chronic wound healing in rats. *Biomed Res Int* 2015; 2015: 846062.
4. Arno AI, Amini-Nik S, Blit PH, et al. Human Wharton's jelly mesenchymal stem cells promote skin wound healing through paracrine signaling. *Stem Cell Res Ther* 2014; 5(1): 28.
5. Chen L, Tredget EE, Wu PY, et al. Paracrine factors of mesenchymal stem cells recruit macrophages and endothelial lineage cells and enhance wound healing. *PLoS ONE* 2008; 3(4): e1886.
6. Sasaki M, Abe R, Fujita Y, et al. Mesenchymal stem cells are recruited into wounded skin and contribute to wound repair by transdifferentiation into multiple skin cell type. *J Immunol* 2008; 180(4): 2581–2587.
7. Sivamani RK, Schwartz MP, Anseth KS, et al. Keratinocyte proximity and contact can play a significant role in determining mesenchymal stem cell fate in human tissue. *FASEB J* 2011; 25(1): 122–131.
8. Zhang J, La X, Fan L, et al. Immunosuppressive effects of mesenchymal stem cell transplantation in rat burn models. *Int J Clin Exp Pathol* 2015; 8(5): 5129–5136.
9. Dominici M, Le Blanc K, Mueller I, et al. Minimal criteria for defining multipotent mesenchymal stromal cells. *Cytotherapy* 2006; 8(4): 315–317.
10. Castro-Manrreza ME, Mayani H, Monroy-Garcia A, et al. Human mesenchymal stromal cells from adult and neonatal sources: a comparative in vitro analysis of their immunosuppressive properties against T cells. *Stem Cells Dev* 2014; 23(11): 1217–1232.
11. Iohara K, Zheng L, Ito M, et al. Side population cells isolated from porcine dental pulp tissue with self-renewal and multipotency for dentinogenesis, chondrogenesis, adipogenesis, and neurogenesis. *Stem Cells* 2006; 24(11): 2493–2503.
12. Li X, Bai J, Ji X, et al. Comprehensive characterization of four different populations of human mesenchymal stem cells as regards their immune properties, proliferation and differentiation. *Int J Mol Med* 2014; 34(3): 695–704.
13. Janmey PA, Winer JP and Weisel JW. Fibrin gels and their clinical and bioengineering applications. *J R Soc Interface* 2009; 6(30): 1–10.
14. Li Y, Meng H, Liu Y, et al. Fibrin gel as an injectable biodegradable scaffold and cell carrier for tissue engineering. *Sci World J* 2015; 2015: 685690.

15. Bruekers SM, Jaspers M, Hendriks JM, et al. Fibrin-fiber architecture influences cell spreading and differentiation. *Cell Adh Migr* 2016; 10(5): 495–504.
16. Ho W, Tawil B, Dunn JC, et al. The behavior of human mesenchymal stem cells in 3D fibrin clots: dependence on fibrinogen concentration and clot structure. *Tissue Eng* 2006; 12(6): 1587–1595.
17. O'Cearbhaill ED, Murphy M, Barry F, et al. Behavior of human mesenchymal stem cells in fibrin-based vascular tissue engineering constructs. *Ann Biomed Eng* 2010; 38(3): 649–657.
18. Steward AJ, Thorpe SD, Vinardell T, et al. Cell-matrix interactions regulate mesenchymal stem cell response to hydrostatic pressure. *Acta Biomater* 2012; 8(6): 2153–2159.
19. Calzada-Contreras A, Moreno-Hernández M, Castillo-Torres NP, et al. Valores de referencia para las pruebas de coagulación en México: utilidad de la mezcla de plasma de donadores de sangre. *Revista Invest Clín* 2012; 64: 437–443.
20. Llames S, Del Río-Nechaevsky M, Larcher F, et al. Human plasma as a dermal scaffold for the generation as a completely autologous bioengineered skin. *Transplantation* 2004; 7: 350–355.
21. Barreda L, Marcet I, Llames S, et al. Human plasma gels: their preparation and rheological characterization for cell culture applications in tissue engineering. *J Mech Behav Biomed Mater* 2019; 89: 107–113.
22. Harunaga JS and Yamada KM. Cell-matrix adhesions in 3D. *Matrix Biol* 2011; 30: 363–368.
23. Rahman A, Carey SP, Kraning-Rush CM, et al. Vinculin regulates directionality and cell polarity in 2D, 3D matrix and 3D microtrack migration. *Mol Biol Cell*. Epub ahead of print 9 March 2016. DOI: 10.1091/mbc.E15-06-0432.
24. Hakkinen KM, Harunaga JS, Doyle AD, et al. Direct comparisons of the morphology, migration, cell adhesions, and actin cytoskeleton of fibroblasts in four different three-dimensional extracellular matrices. *Tissue Eng Part A* 2011; 17(5–6): 713–724.
25. Khetan S, Guvendiren M, Legant WR, et al. Degradation-mediated cellular traction directs stem cell fate in covalently crosslinked three-dimensional hydrogels. *Nat Mater* 2013; 12(5): 458–465.
26. Copland IB, Lord-Dufour S, Cuerquis J, et al. Improved autograft survival of mesenchymal stromal cells by plasminogen activator inhibitor 1 inhibition. *Stem Cells* 2009; 27(2): 467–477.
27. Neuss S, Schneider RK, Tietze L, et al. Secretion of fibrinolytic enzymes facilitates human mesenchymal stem cell invasion into fibrin clots. *Cells Tissues Organs* 2010; 191(1): 36–46.
28. Li G, Zhang XA, Wang H, et al. Comparative proteomic analysis of mesenchymal stem cells derived from human bone marrow, umbilical cord, and placenta: implication in the migration. *Proteomics* 2009; 9: 20–30.
29. Montesinos JJ, Flores-Figueroa E, Castillo-Medina S, et al. Human mesenchymal stromal cells from adult and neonatal sources: comparative analysis of their morphology, immunophenotype, differentiation patterns and neural protein expression. *Cytotherapy* 2009; 11(2): 163–176.
30. Salehinejad P, Alitheen NB, Ali AM, et al. Comparison of different methods for the isolation of mesenchymal stem cells from human umbilical cord Wharton's jelly. *In Vitro Cell Dev Biol Anim* 2012; 48(2): 75–83.
31. Kohli N, Wright KT, Sammons RL, et al. An in vitro comparison of the incorporation, growth, and chondrogenic potential of human bone marrow versus adipose tissue mesenchymal stem cells in clinically relevant cell scaffolds used for cartilage repair. *Cartilage* 2015; 6(4): 252–263.
32. Miranda JP, Filipe E, Fernandes AS, et al. The human umbilical cord tissue-derived MSC population UCX(®) promotes early motogenic effects on keratinocytes and fibroblasts and G-CSF-mediated mobilization of BM-MSCs when transplanted in vivo. *Cell Transplant* 2015; 24(5): 865–877.
33. Li Z, Lee H and Zhu C. Molecular mechanisms of mechanotransduction in integrin-mediated cell-matrix adhesion. *Exp Cell Res* 2016; 349(1): 85–94.
34. Liu Z, Bun P, Auduge N, et al. Vinculin head-tail interaction defines multiple early mechanisms for cell substrate rigidity sensing. *Integr Biol (Camb)* 2016; 8(6): 693–703.
35. Van Tam JK, Uto K, Ebara M, et al. Mesenchymal stem cell adhesion but not plasticity is affected by high substrate stiffness. *Sci Tech Adv Mater* 2012; 13: 064205.
36. Bruekers SMC, Bao M, Hendriks JMA, et al. Adaptation trajectories during adhesion and spreading affect future cell states. *Sci Rep* 2017; 7(1): 12308.
37. Li W, Sigley J, Pieters M, et al. Fibrin fiber stiffness is strongly affected by fiber diameter, but not by fibrinogen glycation. *Biophys J* 2016; 110: 1400–1410.
38. Kim IL, Khetan S, Baker BM, et al. Fibrous hyaluronic acid hydrogels that direct MSC chondrogenesis through mechanical and adhesive cues. *Biomaterials* 2013; 34(22): 5571–5580.
39. Mathieu PS and Loboa EG. Cytoskeletal and focal adhesion influences on mesenchymal stem cell shape, mechanical properties, and differentiation down osteogenic, adipogenic, and chondrogenic pathways. *Tissue Eng Part B Rev* 2012; 18(6): 436–444.
40. Steward AJ, Wagner DR and Kelly DJ. The pericellular environment regulates cytoskeletal development and the differentiation of mesenchymal stem cells and determines their response to hydrostatic pressure. *Eur Cell Mater* 2013; 25: 167–178.
41. Connelly JT, Garcia AJ and Levenston ME. Interactions between integrin ligand density and cytoskeletal integrity regulate BMSC chondrogenesis. *J Cell Physiol* 2008; 217(1): 145–154.
42. Lam J and Segura T. The modulation of MSC integrin expression by RGD presentation. *Biomaterials* 2013; 34(16): 3938–3947.
43. Kapp TG, Rechenmacher F, Neubauer S, et al. A comprehensive evaluation of the activity and selectivity profile of ligands for RGD-binding integrins. *Sci Rep* 2017; 7: 39805.
44. Levy-Beladev L, Levdansky L, Gaberman E, et al. A family of cell-adhering peptides homologous to fibrinogen C-termini. *Biochem Biophys Res Commun* 2010; 401(1): 124–130.
45. Baker BM, Trappmann B, Wang WY, et al. Cell-mediated fibre recruitment drives extracellular matrix mechanosensing in engineered fibrillar microenvironments. *Nat Mater* 2015; 14(12): 1262–1268.
46. Xie J, Bao M, Bruekers SMC, et al. Collagen gels with different fibrillar microarchitectures elicit different cellular responses. *ACS Appl Mater Interfaces* 2017; 9(23): 19630–19637.
47. Hudson NE. Biophysical mechanisms mediating fibrin fiber lysis. *Biomed Res Int* 2017; 2017: 2748340.

48. Cappuzzello C, Doni A, Dander E, et al. Mesenchymal stromal cell-derived PTX3 promotes wound healing via fibrin remodeling. *J Invest Dermatol* 2016; 136: 293–300.
49. Anderson NL and Anderson NG. The human plasma proteome: history, character, and diagnostic prospects. *Mol Cell Proteomics* 2002; 1(11): 845–867.
50. Tahara A, Yasuda M, Itagane H, et al. Plasma levels of platelet-derived growth factor in normal subjects and patients with ischemic heart disease. *Am Heart J* 1991; 122(4 Pt 1): 986–992.
51. Capilla-Gonzalez V, Lopez-Beas J, Escacena N, et al. PDGF restores the defective phenotype of adipose-derived mesenchymal stromal cells from diabetic patients. *Molec Ther* 2018; 26(11): 2696–2709.
52. Hotary KB, Yana I, Sabeh F, et al. Matrix metalloproteinases (MMPs) regulate fibrin-invasive activity via MT1-MMP-dependent and -independent processes. *J Exp Med* 2002; 195(3): 295–308.
53. Lozito TP, Jackson WM, Nesti LJ, et al. Human mesenchymal stem cells generate a distinct pericellular zone of MMP activities via binding of MMPs and secretion of high levels of TIMPs. *Matrix Biol* 2014; 34: 132–143.
54. Acosta L, Hmadcha A, Escacena N, et al. Adipose mesenchymal stromal cells isolated from type 2 diabetic patients display reduced fibrinolytic activity. *Diabetes* 2013; 62(12): 4266–4269.
55. Bongso A and Fong CY. The therapeutic potential, challenges and future clinical directions of stem cells from the Wharton's jelly of the human umbilical cord. *Stem Cell Rev* 2013; 9(2): 226–240.
56. Fajardo-Orduna GR, Mayani H and Montesinos JJ. Hematopoietic support capacity of mesenchymal stem cells: biology and clinical potential. *Arch Med Res* 2015; 46(8): 589–596.
57. Wang Y and Zhao S. Vascular biology of the placenta. San Rafael, CA: Morgan & Claypool Life Sciences, 2010.